Analyzing the Neocortical Fine-Structure

Frithjof Kruggel[1], Martina K. Brückner[2], Thomas Arendt[2], Christopher J. Wiggins[1], and D. Yves von Cramon[1]

[1] Max-Planck-Institute of Cognitive Neuroscience, 04103 Leipzig, Germany
kruggel@cns.mpg.de
[2] Paul-Flechsig-Institute for Brain Research, 04109 Leipzig, Germany

Abstract. Cytoarchitectonic fields of the human neocortex are defined by characteristic variations in the composition of a general six-layer structure. It is commonly accepted that these fields correspond to functionally homogeneous entities. Diligent techniques were developed to characterize cytoarchitectonic fields by staining sections of post-mortem brains and subsequent statistical evaluation. Fields were found to show a considerable interindividual variability in extent and relation to macroscopic anatomical landmarks. With upcoming new high-resolution magnetic resonance (MR) scanning protocols, it appears worthwile to examine the feasibility of characterizing the neocortical fine-structure from anatomical MR scans, thus, defining cytoarchitectonic fields by *in-vivo* techniques.

1 Introduction

There is little doubt regarding a close correspondence between the functional organization of the neocortex and the cytoarchitectonic fields, which have been characterized by different histological staining techniques in post-mortem brains for about the last 100 years [2], [14]. These fields are defined by varying compositions of the general six-layered neocortical fine-structure, which are characterized by the properties and densities of neurons and their connecting fibers. One of the most recent techniques for delineating the borders of cytoarchitectonic fields is called objective cytometry [13]. This technique examines radial intensity profiles across the neocortical sheet in stained brain sections, which are compared statistically along a trajectory on the surface. Local maxima in the classification function indicate a border between two fields.

It is now well accepted these fields show a considerable interindividual variability with respect to macroscopic landmarks (e.g., sulcal and gyral lines and their substructures) [1], [11], [12]. It is an open issue whether macroscopic landmarks (e.g., gyri and sulci) are sufficient for describing the position of functional activation (such as revealed by in-vivo magnetic resonance (MR) scanning), or whether it is necessary to resort to atlas-based descriptions of cytoarchitectonic fields (which are obtained in-vitro from *different* subjects in the form of a probabilistic map).

Recent investigations revealed that a spatial resolution of 0.25 mm for anatomical MRI scanning is feasible. At this resolution, the neocortical sheet is mapped

M.F. Insana, R.M. Leahy (Eds.): IPMI 2001, LNCS 2082, pp. 239–245, 2001.

as a layer of 12 voxels, which may be sufficient to recognize the layer structure of the cortex. Suitable image post-processing techniques may be designed to classify cortical intensity profiles, and thus, to define borders of cytoarchitectonic fields *in-vivo*. Since the MR signal strength is related to the local cellular environment (e.g., biopolymer content) in a volume, it is not unreasonable to assume that stained histological intensity profiles and MR intensity profiles show some similarity (albeit at a much lower spatial resolution). Thus, we will compare previously published results obtained by objective cytometry [15] with a MR-based neocortical fine-structure analysis.

2 Materials and Methods

Brain preparation and scanning: An isolated left brain hemisphere (female, 72 years of age) obtained from an routine autopsy was fixed in 3% formalin and embedded in agar gel. MR acquisition was performed on a Bruker 3 T Medspec 100 system using a T_1-weighted 3D MDEFT protocol [7] (FOV 96x192x128 mm, matrix 256x512x512, voxel size 0.375x0.375x0.25 mm, scanning time 12 h).
Preprocessing: Scan data were interpolated to an isotropical voxel size of 0.25 mm by a fourth-order b-spline method. Intensity inhomogeneities were corrected by a modification of the AFCM [10], yielding a segmentation into three classes (background: BG, grey matter: GM, white matter: WM) and an intensity-corrected version of the input image. The cerebellum and brainstem were manually removed using an image editor and to yield a voxel-based representation of the cerebral WM compartment.
Surface generation: A raw triangular surface was generated from the WM segmentation using the marching tetrahedra algorithm [9] and subsequent mesh optimization to 200k faces [3]. This surface was adaptated to the grey-white matter boundary (WMS) using a deformable model approach [6]. Similarly, a second surface representing the grey matter-background boundary (GMS) was obtained.
Intensity profiles: For each vertex on the WMS, the closest point on the GMS was computed [6]. Along a line through both points, an intensity profile was sampled from the intensity-corrected image at regular intervals of 0.1 mm. In order to define the WM-GM and GM-BG boundary points consistently, lines were adaptated to the rising flank of the profile (at the GM-WM boundary) and to the falling flank (corresponding to the GM-BG boundary, see Fig. 1). The exact position of the GM-WM boundary was determined at intensity $I = 135$ (GM-WM-boundary at $I = 100$), and their distance was recorded as the local cortical thickness th. Because layers are found at a rather constant *relative* position within the cortex, profiles were resampled at 1% intervals of th. Thus, we obtained for each vertex on the WMS the cortical thickness and a normalized intensity profile of 101 data points. *Modeling profiles:* Intensity profiles were characterized for statistical evaluation by (i) the slope of the rising flank at the GM-WM boundary m_0 (see Fig. 1), (ii) the slope of the intra-cortical portion m_1, (iii) the slope of the falling flank at the GM-BG boundary m_2. In addition,

the position (bp), intensity (bi) and width (bw) of an intra-cortical band were determined by adaptation of a Gaussian function to the intra-cortical profile segment.

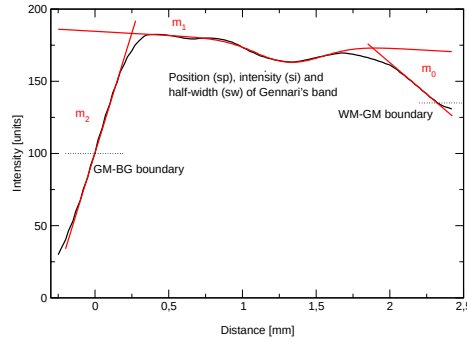

Fig. 1. Example intensity profile across Area 17. The rising flank (on the left) crosses the WM-GM border, whereas the slope of the intra-cortical segment is comparatively flat. The falling flank mostly results from the partial volume effect on the GM-BG boundary. A Gaussian function is used to model the position, intensity and width of intra-cortical bands, such as Gennari's band.

Statistical evaluation: Cortical areas with similar fine structure were determined by comparing profile properties of a template region with a local cortical patch. For the template, profile properties were collected from a surface patch of 5 mm diameter centered in a region of interest (typically 60-100 vertices). Properties of the test region were sampled from a given vertex and its first and second-order neighbors (typically 10-30 vertices). Six statistical tests were heuristically selected to measure the similarity between both regions: (z_1) Pearson's correlation coefficient of the averaged profile in both regions, (z_2) Pearson's correlation coefficient of the first derivative of the averaged profiles, (z_3) a t-test comparing the cortical thickness th, (z_4) a t-test comparing the rising slope m_0, (z_5) a t-test comparing the intra-cortical slope m_1, and (z_6) a t-test comparing the band intensity bi. As indicated, tests measures were converted into z-scores, and a similarity measure was derived as: $z_{sim} = z_1 + z_2 - |z_3| - |z_4| - |z_5| - |z_6|$. If both regions contain similar profiles, z_3-z_6 contribute values close to 0, while z_1 and z_2 provide positive scores, summing up to some (small) positive quantity. For dissimilar regions, negative similarity measures are expected. A (heuristically derived) threshold of $z_{sim} \geq -1$ was used in all subsequent figures.

3 Results

We selected three different anatomical regions which are well studied by histological techniques. We were interested in comparing intensity profiles with the

known descriptions of local layer structure, and in comparing the extent of statistically homogeneous regions with known cytoarchitectonic fields. Note that the T_1 contrast is "inverted" by fixation: regions of higher neuron content (i.e., cortical layers 1-3, 5 and 6, basal ganglia) show a higher signal intensity than fiber-containing regions (i.e., the white matter).

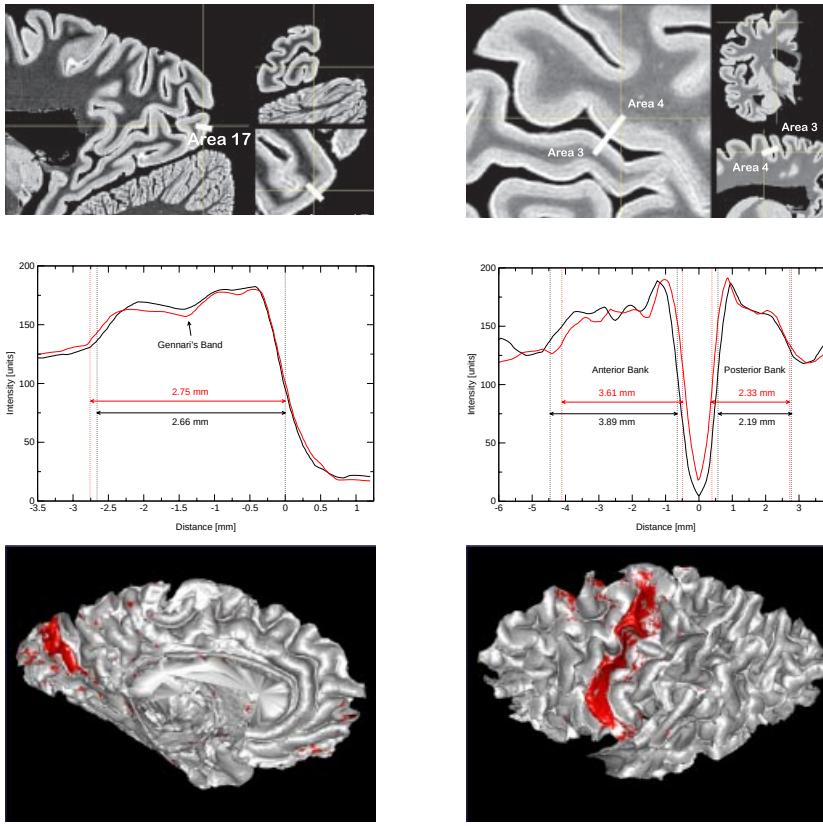

Fig. 2. Left: A sample profile through the visual cortex reveals Gennari's band as an intensity drop at $\approx$ 52 % of the cortical width. A region is detected by statistical classification which compares well with neuroanatomical knowledge. Right: A sample profile through the anterior (Area 4, motor cortex) and posterior (Area 3, sensory cortex) bank of the central sulcus. Using a spot at Broca's knee as a template, a region is detected which is similar in extent to the motor cortex.

Visual Cortex (Area 17): The visual cortex is distinguishable from the surrounding Area 18 by the presence of Gennari's band, which corresponds to an intracortical horizontal fiber system. This structure is easily detected in the acquired MR dataset as a darker band in the bright cortex (see Fig. 2, top left).

The cortical thickness on the banks of the calcarine fissure were determined as 1.86±0.10 mm ([15]: 1.84 mm), the position of the center of Gennari's band as 52±6 % ([15]: 55 %), and the thickness of this band as 0.30± 0.10 mm ([15]: 0.28 mm). According to von Economo [14], Area 17 is located on the walls and lips of the calcarine fissure, and at the gyral crowns at the occipital pole. This description compares nicely with the automatically generated statistical classification as shown in Fig. 2, bottom left.

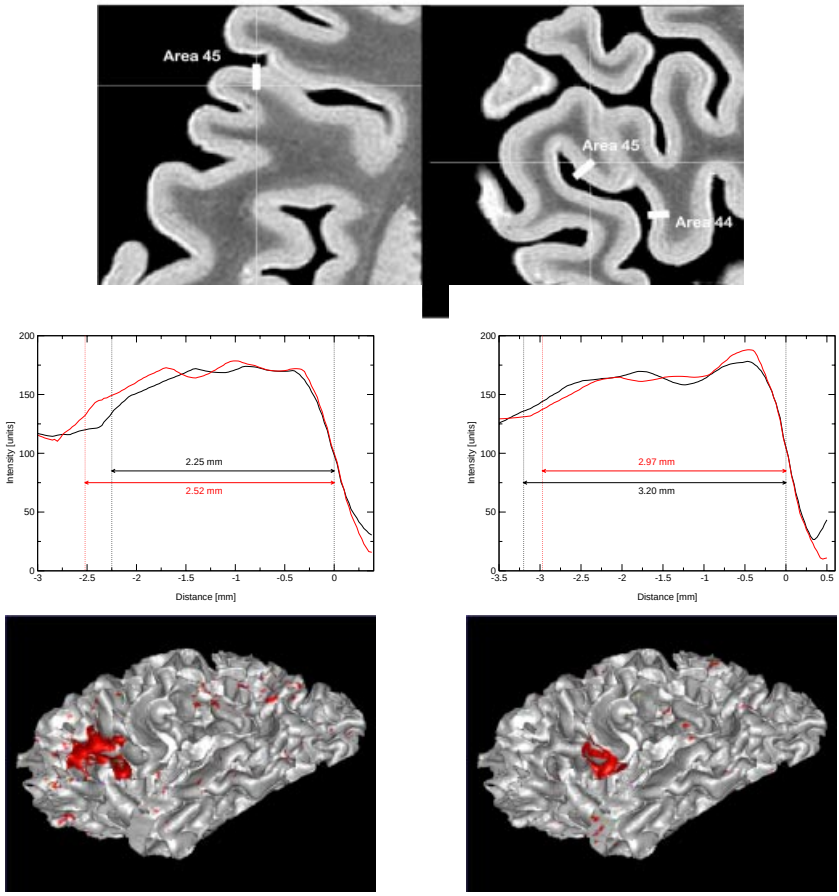

Fig. 3. Top: Axial (enlarged) and sagittal section through the inferior frontal gyrus. Profile were taken from the *pars triangularis* (Area 45) and the *pars opercularis* (Area 44). The cortex is thinner in Area 45, but exhibits a more prominent banded structure. Lateral view of the white matter surface. Area 45 (left) and Area 44 (right) were detected from model position shown above.

Motor and Sensory Cortex (Area 4 and 3): Next, we tried to differentiate the primary motor cortex (Area 4) on the anterior bank of the central sulcus from the somatosensory cortex (Area 3) on its posterior bank (see Fig. 2, top right). The most distinctive feature here is the cortical thickness: on the anterior bank, the motor cortex reaches values up to 3.8 mm, compared to less than 2.2 mm for the sensory cortex [8]. Intensity profiles in Area 4 mostly showed three maxima (see Fig. 2, middle right), which roughly correspond to the transition between layer II/III, layer III/V and layer V/VI as described by Amunts et al. [1]. The somatosensory cortex on the posterior bank exhibited much less substructure. A statistical classification was initialized by a manually specified region close to the hand field and yielded the full extent of the motor cortex well in agreement with previously published histological classifications (see Fig. 2, bottom right).

Broca's Area (Area 44 and 45): As a final example, we selected Broca's speech region, which corresponds to Area 44 (the pars opercularis of the inferior frontal gyrus) and Area 45 (the pars triangularis of the inferior frontal gyrus). As described by Amunts et al. [1], the cortex of Area 44 is not sharply delineable from the white matter, which corresponds to a flat slope of m_0 (see Fig. 3, middle right). The cortex of Area 45 (see Fig. 3, middle left) is thinner and features a more distinct horizontal layering. Classification results are shown superimposed on the white matter surface, separated for Area 45 (bottom left) and Area 44 (bottom right).

4 Discussion

Results shown for three different brain areas demonstrate the feasibility of analyzing the neocortical substructure from high-resolution MR data. The qualitative properties of the MR intensity profiles and quantitative descriptors (e.g., cortical thickness, band position and width) corresponded well with descriptions found in reference publications based on histological examinations. Using statistical descriptors of the profiles obtained from a template region, the extent of target regions was determined by comparing local descriptors with the template. Regions found correspond well with prior knowledge from histological examinations. There is a striking qualitative similarity of our MR intensity profiles with photometric studies of the myeloarchitecture [4], and theoretical studies [5] demonstrated the equivalence of Nissl-stained cytometric intensity profiles with Weigert-stained myelin profiles. Although the spatial resolution of the our MR data is at least one order of magnitude lower than traditional histological techniques results suggest that perhaps a microscopic resolution is not required if a classification of cortical areas is sought for. However, at a higher resolution (say, 0.1 mm), even more detail might be revealed, thus leading to more powerful statistical classifiers.

We want to emphasize the preliminary nature of this feasibility study. First of all, the validation of our regional classification by histological examination of the same specimen is missing. It is an open issue how much the approach

described here may be translated to in-vivo studies, given the limited scanning time when examining test subjects and unavoidable motion artefacts.

The possibility of studying the neocortical fine-structure by MR imaging, i.e., introducing a myeloarchitecture-related parcellation of an individual brain, offers exciting perspectives for the analysis of structure-function relationships in the brain on a mesoscopic level.

References

1. Amunts, K., Schleicher, A., Bürgel, U., Mohlberg, H., Uylings, H.B.M., Zilles, K.: Broca's region revisited: cytoarchitecture and intersubject variability. J. Comp. Neurol. **412** (1999), 319–341.
2. Brodmann, K.: Die vergleichende Lokalisationslehre der Grosshirnrinde. Barth, Leipzig (1909).
3. Garland, M., Heckbert, P.S. Optimal triangulation and quadric-based surface simplification. J. Comp. Geom. **14** (1999), 49–65.
4. Hopf, A.: Registration of the myeloarchitecture of the human frontal lobe with an extinction method. J. Hirnforschung **10** (1968), 259–269.
5. Hellwig, B.: How the myelin picture of the human cerebral cortex can be computed from cytoarchitectonic data. A bridge between von Economo and Vogt. J. Hirnforschung **34** (1993), 387–402.
6. Kruggel, F., von Cramon D.Y.: Measuring the neocortical thickness. In: Mathematical Methods in Biomedical Image Analysis (Hilton Head), pp. 154-161. IEEE Press, Los Alamitos (2000).
7. Lee, J.H., Garwood, M., Menon, R., Adriany, G., Andersen, P., Truwit, C.L., Ugurbil, K.: High contrast and fast three-dimensional magnetic resonance imaging at high fields. Magn. Reson. Med. **34** (1995), 308–312.
8. MacDonald, D, Kabani, N., Avis, D., Evans, A.C.: Automated 3-D extraction of inner and outer surfaces of cerebral cortex from MRI. Neuroimage **12** (2000), 340–356.
9. Payne, B.A., Toga, A.W.: Surface mapping of brain function on 3D models. IEEE CGA **10** (1990), 33–41.
10. Pham, D.L., Prince J.L.: An adaptive fuzzy segmentation algorithm for three-dimensional magnetic resonance images. In: Information Processing in Medical Imaging (IPMI'99), LNCS **1613**, pp. 140–153. Springer, Heidelberg (1999).
11. Rademacher, J., Caviness, V.S., Steinmetz, H., Galaburda, A.M.: Topographical variation of the human primary cortices: implications for neuroimaging, brain mapping and neurobiology. Cereb. Cortex **3** (1995), 313-329.
12. Rajkowska, G., Goldman-Rakic, P.S.: Cytoarchitectonic definition of prefrontal areas in the normal human cortex: II. Variability in locations of areas 9 and 46 and relationship to the Talairach coordinate system. Cereb. Cortex **5** (1995), 323–337.
13. Schleicher, A., Zilles, K.: A quantitative approach to cytoarchitectonics: analysis of structural inhomogeneities in nervous tissue using an image analyzer. J. Microscopy **157** (1990), 367–381.
14. von Economo, C.: Zellaufbau der Grosshirnrinde des Menschen. Springer-Verlag, Wien (1927).
15. Zilles, K., Werners, R., Büsching, U., Schleicher, A.: Ontogenesis of the laminar structure in areas 17 and 18 of the human visual cortex. Anat. Embryol. **174** (1986), 339–353.